



**HAL**  
open science

## Rheological properties and stability of Pickering emulsions stabilized with differently charged particles

Mathis Benyaya, Marie-Alexandrine Bolzinger, Yves Chevalier, Claire Bordes

► **To cite this version:**

Mathis Benyaya, Marie-Alexandrine Bolzinger, Yves Chevalier, Claire Bordes. Rheological properties and stability of Pickering emulsions stabilized with differently charged particles. *Colloids and Surfaces A: Physicochemical and Engineering Aspects*, 2024, 687, pp.133514. 10.1016/j.colsurfa.2024.133514 . hal-04475960

**HAL Id: hal-04475960**

**<https://hal.science/hal-04475960>**

Submitted on 23 Feb 2024

**HAL** is a multi-disciplinary open access archive for the deposit and dissemination of scientific research documents, whether they are published or not. The documents may come from teaching and research institutions in France or abroad, or from public or private research centers.

L'archive ouverte pluridisciplinaire **HAL**, est destinée au dépôt et à la diffusion de documents scientifiques de niveau recherche, publiés ou non, émanant des établissements d'enseignement et de recherche français ou étrangers, des laboratoires publics ou privés.

# Rheological properties and stability of Pickering emulsions stabilized with Differently Charged Particles

Mathis Benyaya, Marie-Alexandrine Bolzinger, Yves Chevalier\*, Claire Bordes\*

*Université Claude Bernard Lyon 1, CNRS UMR 5007, Laboratoire d'Automatique, de Génie des Procédés et de Génie Pharmaceutique (LAGEPP), 43 bd du 11 Novembre 1918, 69622 Villeurbanne, France.*

**Authors and contact:** Mathis Benyaya [mathis.benyaya@univ-lyon1.fr](mailto:mathis.benyaya@univ-lyon1.fr)  
Marie-Alexandrine Bolzinger [marie.bolzinger@univ-lyon1.fr](mailto:marie.bolzinger@univ-lyon1.fr)  
Yves Chevalier \* [yves.chevalier@univ-lyon1.fr](mailto:yves.chevalier@univ-lyon1.fr)  
Claire Bordes \* [claire.bordes@univ-lyon1.fr](mailto:claire.bordes@univ-lyon1.fr)

\*: *corresponding authors*

**Keywords.** Pickering emulsions, Rheology, Coalescence, Formulation, Stability

## Highlights

- Droplet morphology influences both rheology and stability of Pickering emulsions.
- High particle surface coverage of droplets decreases the storage modulus.
- High particle surface coverage of droplets increases their stability.
- Thermal ageing and forced coalescence stability measurements are consistent.
- Mixed oppositely charged particles as emulsifiers improve the emulsion stability.

## Abbreviations

**A-PMMA:** Anionic PMMA-like copolymer, similar abbreviation was used for neutral (N-PMMA) and cationic (C-PMMA) copolymers.

**a-PMMA:** Particles obtained from A-PMMA copolymer, similar abbreviations were used for n- and c-pmma particles.

**A-emulsion:** Emulsion stabilized with a-PMMA particles, similar abbreviations were used for N- and C-emulsions.

**A/C-emulsion:** Emulsion prepared with mixed anionic and cationic particles, similar abbreviations were used for A/N- and N/C-emulsions. When no precision is given, the mixture composition is 50/50 w/w.

**MTPs:** Mono-Type Particles emulsions refer to as A-, N- and C-emulsions.

**DCPs:** Differently Charged Particles emulsions refer to as A/C-, A/N-, and N/C-emulsions.

**Abstract**

The formulation of Pickering emulsions is a major challenge in many industrial areas. The impact of the formulation of o/w Pickering emulsions on their stability and rheological properties is addressed, with emphasis given on the influence of the types of solid particles ensuring droplet stabilization. Three differently charged polymer microparticles (neutral, anionic and cationic) are used alone or as their binary mixtures to investigate the influence of the particles charges on the rheological behavior and stability of concentrated o/w emulsions, together with the possible synergies with mixed particles. The morphology and the coverage of the droplets by particles are two important factors influencing both the rheological properties and the stability of the emulsions. The benefits of using a charge-stoichiometric mixture of anionic and cationic particles as emulsifiers to efficiently prevent the destabilization mechanisms are also highlighted.

## 1. Introduction

For environmental reasons, the design of surfactant-free emulsions is a major challenge for many industrial applications. In this context, Pickering emulsions are a promising way forward, but more knowledge is needed to design and control their properties. In particular, the effect of the formulation parameters on the rheological properties and the stability of these emulsions is a major matter of concern.

Pickering emulsions are emulsions stabilized by solid colloidal particles rather than surfactant molecules. The colloids are irreversibly adsorbed at the oil/water interface, conferring the emulsions some unique properties such as very high stability against coalescence and thermal treatments [1]. The irreversible adsorption of particles is revealed by the linear dependence of the droplet diameter on the particle concentration [2]. Due to their very strong adsorption, particles densely pack at the droplet surface, so that the main contribution to emulsion stabilization is the formation of a rigid adsorbed layer of solid particles that prevents droplet coalescence. When a stress is applied to make the emulsion flow, the droplets deform into an elongated shape for they can slide over each other and align along the flow. The energy required to deform the droplets and align them is related to the values of its storage and loss moduli.

The nature of both the particulate emulsifier [3,4] and the liquid phases [5] influence the rheological properties of such emulsions. The droplets of Pickering emulsions are more rigid than those of classical emulsions [6]. The influence of the different formulation parameters on the rheological properties of Pickering emulsions remains complex to infer. In general, concentrated Pickering emulsions are described as having the elastic behavior of a 3D network.

The first general feature is that the viscoelastic properties of a dispersion are mostly controlled by those of the continuous phase. But two other phenomena influence the viscoelastic properties of Pickering emulsions during a deformation in a flow.

The first phenomenon involves attractive interactions that can occur between particles in the continuous aqueous phase, leading to the formation of a network of droplets or particles. Hence, emulsions can act as a 3D network with elastic behavior. This first effect is particularly important in Pickering emulsions where particles are often in large excess compared to the oil-water interfacial area to be covered, thus forming a network between the droplets in the aqueous phase [1,7], or where a high salt concentration causes flocculation of the particles [4,7–9].

The second phenomenon is the droplet deformation itself [10]. This is specific to concentrated emulsions. When subjected to a stress, the droplets deform and align in the flow, increasing the viscous response. Frith *et al.* [11] showed that at high oil volume fractions,  $\Phi > 0.60$ , the salt concentration does not affect the rheology of Pickering emulsions stabilized by silica particles, suggesting a weak role of electrostatic interactions between particles in the aqueous phase and a higher importance of the droplet deformation. More information on the effect of particle flocculation on the rheology of emulsions has been obtained by studies of the rheology of the silica particle suspensions showing that particle aggregation and formation of

a 3D network only occurred at high salt concentrations [12,13]. However, it is difficult to infer the relative importance of droplet deformation and particle interactions in the rheological behavior of Pickering emulsions. To address this issue, Katepalli *et al.* [12] considered the dimensionless capillary number and elastocapillary number of the system as a framework. The capillary number  $Ca$  compares the force required to flow the emulsion with the force required to deform a single droplet. The elastocapillary number  $Ca_G$  compares the force required to cause elastic deformation of the emulsion with the force required to deform a single droplet. They are defined as

$$Ca = \frac{\mu_e \dot{\gamma} d}{\sigma} \quad (\text{Eq. 1})$$

$$Ca_G = \frac{G' d}{\sigma} \quad (\text{Eq. 2})$$

Where  $\mu_e$  is the shear rate viscosity,  $\dot{\gamma}$  is the shear rate,  $G'$  is the storage modulus,  $d$  is the droplets diameter, and  $\sigma$  is the interfacial tension between water and oil. If  $Ca_G \ll 1$ , the droplets unlikely deform under the applied stress. Conversely, if the forces are of similar magnitude, i.e.  $Ca_G \approx 1$ , the droplets can easily deform [12,14,15]. However, the relevance of the elastocapillary number is lost when the emulsion structure is broken beyond the yield stress.

In terms of emulsion stability, many phenomena have been considered as destabilizing mechanisms including coagulation, coalescence, Ostwald ripening, but also creaming. Although creaming makes emulsions inhomogeneous, it is not a real loss of stability because the oil droplets remain intact in the creamed layer. Ostwald ripening only occurs for very fine nanoemulsions when the curvature of the oil droplets is high. The main mechanisms to be considered are coagulation and coalescence. Coalescence is the actual destabilization mechanism by which droplets merge, and are finally released into a macroscopic layer of pure oil on top of the emulsion. In efficiently stabilized emulsions, the loss of stability is difficult to detect because it is very slow. For large enough droplets (more than 1  $\mu\text{m}$  diameter), creaming is fast, so that creaming goes to completion before coalescence can start. Consequently, coalescence takes place in the creamed layer, whatever the concentration of the emulsions. It is therefore advisable to investigate the stability of emulsions, either in a concentrated state or within the creamed layer, even if the emulsion of actual interest is dilute. No definite protocol has been given as a standard for the evaluation of the stability of Pickering emulsions but several techniques have been used to accelerate the destabilization. The earliest and most common accelerated ageing test consists in the storage of the emulsion at different temperatures for several months. Application of various types of destabilizing stimuli causing coalescence allows faster assessment of emulsion stability. In particular, centrifugation has been shown to be correlated with the thermal stability of surfactant-based emulsions (ISO/TR 18811). Comparison between thermal ageing coalescence and centrifugation-induced coalescence has been made for classical emulsions, but not, as far as we know, for Pickering emulsions. It is worth studying the case of Pickering emulsions because the stabilization mechanisms by adsorbed particles is different of that of surfactants. The stability of classical and Pickering emulsions has been also assessed by rheology measurements [16–18].

This work follows a previous study of surface coverage by adsorbed particles and droplet size of o/w Pickering emulsions stabilized by neutral, anionic or cationic particles and their mixtures [19]. It was shown that the adsorption rate of the particles at the water-oil interface during the emulsification process strongly influences the organization of the particles at the droplet surface and thus emulsions characteristics. The present approach is to analyze the rheological properties and the stability against coalescence of the same Pickering emulsions in order to obtain deeper information about their structure and the interactions between droplets. The stability of the different emulsions against coalescence was also studied both by a thermal ageing test and by a forced coalescence under centrifugation. The possibility of using forced coalescence as a predictive method for stability under the thermal ageing of Pickering emulsions was discussed. Finally, the results were compared and related to the emulsion droplet coverage and size.

## **2. Materials and methods**

### 2.1. Materials

Methyl methacrylate (MMA, purity  $\geq 99.0\%$ ) from Sigma-Aldrich, methacrylic acid (purity  $\geq 99.5\%$ ) (MAA) from Acros Organics, hydroxyethyl methacrylate (HEMA) from Sigma-Aldrich, and 2-(dimethylamino)ethyl methacrylate (DMAEMA) from Sigma-Aldrich were used as monomers to synthesize the copolymers used for the formulation of the particles. The different solvents used during these syntheses were tetrahydrofuran (THF, purity  $\geq 99.0\%$ ) purchased from Sigma-Aldrich and heptane (purity  $\geq 99.0\%$ ) from VWR Chemicals. 2,2'-Azobis(2-methylpropionitrile) (AIBN) from Sigma-Aldrich was used as an initiator of the polymerization reaction.

Ethyl acetate (purity  $\geq 99.5\%$ ) from Sigma was used as the organic phase for the formulation of the particles. The fluorophores encapsulated were Nile red purchased from TCI and ATTO 425 NHS-Ester purchased from Atto-tec.

The poly(vinyl alcohol) (PVA) Mowiol 4-88 purchased by Sigma-Aldrich was used as the emulsifier for the particle preparation.

A classical cosmetic oil was used to prepare the o/w emulsions was chosen: isononyl isononanoate supplied by Stéarinerie Dubois.

### 2.2. Polymer synthesis and characterization

"PMMA-like" copolymers were synthesized with more than 90 wt% of monomers being MMA and the comonomer being neutral, anionic or cationic. MAA, HEMA and DMAEMA were respectively used to synthesize anionic, neutral and cationic copolymers respectively called A-PMMA, N-PMMA and C-PMMA. The synthesis was a free-radical copolymerization process at 60 °C in THF solution using AIBN as initiator. Anionic PMMA (A-PMMA) was obtained by combining MMA and MAA monomers at 95/5 weight ratio. Neutral PMMA (N-PMMA) was obtained by combining MMA and HEMA monomers at 95/5 weight ratio. Cationic PMMA (C-PMMA) was obtained by combining MMA and DMAEMA monomers at 90/10 weight ratio.

This latter ratio was chosen differently in order to obtain enough charges at the surface of the final particles. The polymerization recipe contained 15 g of monomers in 300 mL of THF under nitrogen flow to prevent deactivation of radicals by oxygen. 0.3 g of AIBN initiator was added into the deoxygenated monomer solution at 60 °C for starting the free radical polymerization reaction. After 5 h, the mixture was left to cool down to room temperature, and the solution was poured dropwise into a large amount of heptane under vigorous stirring for precipitation of the copolymers. More details are given in [19]. These copolymers were then used to prepare microparticles.

### 2.3. Particles formulation and characterization

#### **2.3.1. Particles formulation**

PMMA-like microparticles were obtained by the emulsion/evaporation technique. 1.25 g polymer was dissolved in 10 mL of ethyl acetate and mixed with a PVA aqueous solution. Then, after the emulsification, 150 mL of water was added and the organic solvent was let to evaporate at room temperature during 4 h.

For the preparation of neutral PMMA particle suspension, the emulsion was obtained by mixing the organic phase and a 1.2 wt% PVA solution with an Ultra-Turrax device at 24 000 rpm for 5 min. For anionic PMMA particles, emulsification was performed using an ultrasound probe at 70% for 2 min using a 1.2 wt% PVA solution. For cationic particles, a 0.4 wt% PVA solution was used and the emulsion was prepared with an Ultra-Turrax device at 17 500 rpm for 5 min. These different operating conditions were necessary to obtain particles with a similar size of about 1 μm. Eight washing steps were then applied to the particle suspensions in order to remove PVA [20]. In the full article, a-PMMA refers to “particles obtained from A-PMMA polymer”. The same abbreviations were used for cationic (c-PMMA) and neutral particles (n-PMMA).

#### **2.3.2. Particles characterization**

The particle concentration in the obtained suspensions was determined by measuring the dry extract mass. Measurements were performed in triplicate for each suspension.

The particles size distributions were measured in triplicate by small-angle light scattering using a Malvern Mastersizer 3000 instrument (Malvern Instruments Ltd, UK). The used real part of the refractive index was that of PMMA (1.49) and its imaginary part was zero for all the particles. The measurements were made in triplicate at a stirring rate in the sample dilution beaker of 1400 rpm. The size distribution was expressed as its median diameter  $D(50)$  and

$$span = \frac{D(90) - D(10)}{D(50)}.$$

ζ-potential is a good indicator of the electric charge of the particles. It was determined using a Zetasizer NanoZS (Malvern Panalytical, France) at neutral pH and 20 °C. The ionic strength was adjusted with NaCl for the conductivity was 1 mS·cm<sup>-1</sup>.

## 2.4. Emulsion formulation and characterization

### **2.4.1. Emulsions formulation**

The suspensions of polymer particles were diluted with water until obtaining 8 g of suspension at a given particle concentration. Emulsions were prepared by mixing 2 g of oil and the aqueous suspension with an Ultra-Turrax mixer at two different stirring rates and durations: at 24 000 rpm for 6 min or at 6 500 rpm for 20 min. These emulsions were made with either a single type of particles (Mono-Type Particles (MTP) emulsions) or a mixing with a 50/50 w/w ratio of two different particles (Differently-Charged Particles (DCP) emulsions). For the rest of the article, “emulsion made from a-PMMA” is denoted as A-emulsion. The same denomination is used for C-emulsion and N-emulsion. A/C-emulsion designates an emulsion made with a 50/50 mixture of anionic and cationic particles. Same denomination is used for A/N-emulsion and N/C-emulsion.

Three concentrations of particles were used 21, 32 and 43 mg of particles per cm<sup>3</sup> of oil. 36 different emulsions were prepared.

### **2.4.2. Emulsions characterization**

#### *Droplets median diameter and coverage*

The droplet size was determined by analyzing optical microscopy images collected at x100 magnification of the objective of a Leica DMLM microscope. For this purpose, the software ImageJ was used to measure the diameter of 100 droplets in each prepared emulsion. The median diameter was taken as a measurement of the droplets size.

The particles coverage of the droplets, defined as the fractional area of droplet covered by particles, was calculated as:

$$Coverage = \frac{d_a c_p}{4 \rho d_p} \quad (Eq. 3)$$

A coverage of 100% means that all the surface area of the droplet is covered by particles. In the case of monodisperse spherical particles, the highest coverage that can be geometrically reached is 91%.

#### *Volume fraction of oil in aqueous phase*

To determine the oil volume fraction  $\Phi$  in an emulsion, the emulsion was let creaming and a sample of the cream was dried at 45 °C during 6 h. The mass after drying is the mass of oil and particles initially present in the emulsion. It was divided by the initial mass of the sample to determine  $\Phi$ . The mass of the dried sample was kept identical after 6 h or 24 h, showing that only and all the water has evaporated.

#### *Rheological properties of the emulsions*

The rheological measurements were made on concentrated emulsions at 25 °C with an Anton Paar MCR302 rheometer. As creaming was very fast, the sample was let undergoing creaming in a pipette and the aqueous part was eliminated before the deposition of the concentrated emulsion onto the rheometer plate. Similar protocol was used for Pickering emulsions with large droplets [11].



A frequency sweep test was performed at a shear strain of 0.05%, within the viscoelastic linear region previously determined by an amplitude sweep test. A plane-plane geometry of 25 mm diameter and a gap of 1 mm was used. The frequency was decreased from 100 down to 0.1 rad s<sup>-1</sup>. Two parameters were measured, the storage modulus  $G'$  and the loss modulus  $G''$ .  $G'$  was used for the calculation of the elastocapillary number  $Ca_G$  (Eq. 2).

Shear viscosity measurements were also performed with a shear rate increasing from 0.01 s<sup>-1</sup> to 1000 s<sup>-1</sup> with the same geometry.

### Thermal ageing of emulsions

As already observed in [19], no destabilization of the emulsions was observed after 6 months of storage at room temperature. Therefore, a heat-ageing test was used to accelerate the destabilization process. No standard method is currently available, so that reported storage temperature and duration vary from one literature source to another. Thermal ageing tests typically last several months at low (0 °C), ambient (25 °C) or medium-high temperatures (e.g. 50 °C) [21,22]. 50 °C is the highest temperature used for accelerated ageing; higher temperatures may be used to test the thermal stability of a product [23]. The emulsions tested were stored at 45 °C for seven months and visually characterized. This protocol was used to characterize the 24 emulsions containing 21 or 43 mg of particles per cm<sup>3</sup> of oil.

### Stability of the emulsion against stress

Forced coalescence refers to the act of applying a pressure to the emulsion to accelerate the destabilization mechanisms, especially coalescence. In general, the emulsion is centrifuged at high speed [24–26]. The sum of the centrifugal and buoyancy forces acting against each other pushes the emulsion droplets against each other, causing the biggest droplets to coalesce [27]. This may lead to the release of a supernatant oil layer.

The stability of the emulsions was analyzed using a Dispersion Analyser LUMiSizer® (LUM GmbH, Berlin, Germany). As there is a large excess of water in the formulations, the samples were allowed to cream before being placed in a 10 mm polycarbonate cell and subjected to centrifugation at 4 000 rpm for 1 h at 20 °C. Throughout the experiment, the sample was illuminated by a laser light and the transmitted light was measured over its entire height. At the end of the experiment, some oil may have been released from the emulsion and a separation index was defined as the ratio between the thickness of the released oil layer and the initial height of the emulsion. This was calculated by using the SEPView® software of the instrument.

### 3. Results

#### 3.1. Physicochemical properties of the particles and emulsions

Due to the robustness of the methodology used for Pickering emulsion preparation, the physicochemical properties of the three types of particles (a-, c- and n-PMMA) and the six types of emulsions (A-, C-, N-, A/C-, N/C- and N/A-emulsions) were similar to the previously published results [20]. These properties are briefly summarized in the following section.

##### 3.1.1. Particle median size and charge

Dry extract measurements indicated that the particle concentration after synthesis was about 2 wt% in all types of suspensions. The particle median size  $D(50)$  was around 1  $\mu\text{m}$  (Table 1).

**Table 1.** Median size of the three different particle suspensions ( $n = 3$ ).

Particles	$D(50)$ (nm)	SEM (nm)	Span
a-PMMA	991	4	1.63
n-PMMA	634	3	1.14
c-PMMA	1067	42	1.15

The  $\zeta$ -potential measured for the n-PMMA particles was around 0 mV, as expected for neutral particles. For a-PMMA and c-PMMA particles, the  $\zeta$ -potential was similar in absolute value (resp.  $-11$  mV and  $+11 \pm 2$  mV). As their  $\zeta$ -potential value and the median size were identical, these two particle types had similar surface charge densities. Therefore, a 50/50 w/w mixture of these particles resulted in a neutral mixture.

##### 3.1.2. Physicochemical properties of the emulsions

The ratio of particle mass to oil volume is a very important parameter in the development of Pickering emulsions [28]. Here, three different particle concentrations were used (42.6, 31.9 and 21.3 mg of particles per  $\text{cm}^3$  of oil) while the oil amount was kept at 20 wt%. It has previously been shown that such a variation of particle concentration had no significant effect on the droplet surface coverage and that no free particles remained in suspension in the continuous aqueous phase [19]. Emulsions were prepared at two different stirring rates by using an Ultra-Turrax device rotating at either 24 000 rpm or 6 500 rpm. Table 2 reports the droplet median diameter and the resulting coverage for all the prepared emulsions. Depending on the operating conditions, the droplet size varied between 60 and 200  $\mu\text{m}$  and the coverage between 60% and 90%. The emulsions prepared at 6 500 rpm showed higher coverage than those prepared at 24 000 rpm. As analyzed in more details in our previous study [20], there were two exceptions to this trend. At high stirring rates, the coverage of A-emulsions reached the maximum theoretical value corresponding to the full coverage of a 2D surface by spherical particles, i.e. 91%. Therefore, the droplet coverage cannot be increased by reducing the stirring rate. The same applies to the droplet diameters. A/C-emulsions made at 6 500 rpm had a lower coverage because of the presence of particle aggregates during the emulsification.

Measurements were performed on the creamed layer made of a concentrated emulsion. Indeed, the destabilization by coalescence takes place in the creamed layer. As  $\Phi$  is a major factor influencing the viscosity of emulsions [14,29], it was measured for all 6 types of emulsions. The oil volume fractions  $\Phi$  were all around 56% indicating highly concentrated emulsions and no statistically significant difference was found between them. The concentration of particles, the type of particles and the stirring conditions did not change the value of  $\Phi$ .

**Table 2.** Median diameter and surface coverage of the emulsion droplets obtained with different types and concentrations of particles. Results are presented as Median  $\pm$  SEM for the droplet diameter ( $n = 3$ ) and as Mean  $\pm$  SEM for the droplet coverage ( $n = 3$ ).

Emulsion type	Stirring rate (rpm)	Droplet median diameter ( $\mu\text{m}$ )			Coverage (%)
		21 $\text{mg}\cdot\text{cm}^{-3}$	32 $\text{mg}\cdot\text{cm}^{-3}$	43 $\text{mg}\cdot\text{cm}^{-3}$	
A-	24 000	195 $\pm$ 5	137 $\pm$ 4	97 $\pm$ 3	90 $\pm$ 3
	6 500	193 $\pm$ 4	134 $\pm$ 4	91 $\pm$ 3	88 $\pm$ 3
N-	24 000	98 $\pm$ 2	68 $\pm$ 2	60 $\pm$ 2	83 $\pm$ 2
	6 500	110 $\pm$ 3	80 $\pm$ 2	47 $\pm$ 2	70 $\pm$ 2
C-	24 000	142 $\pm$ 3	92 $\pm$ 3	71 $\pm$ 2	59 $\pm$ 2
	6 500	156 $\pm$ 2	100 $\pm$ 1	77 $\pm$ 1	65 $\pm$ 1
A/N-	24 000	142 $\pm$ 4	90 $\pm$ 1	70 $\pm$ 1	77 $\pm$ 2
	6 500	150 $\pm$ 3	96 $\pm$ 1	81 $\pm$ 2	85 $\pm$ 2
N/C-	24 000	114 $\pm$ 3	75 $\pm$ 2	60 $\pm$ 1	61 $\pm$ 2
	6 500	142 $\pm$ 3	90 $\pm$ 3	78 $\pm$ 2	76 $\pm$ 3
A/C-	24 000	163 $\pm$ 4	110 $\pm$ 2	81 $\pm$ 2	71 $\pm$ 2
	6 500	140 $\pm$ 3	93 $\pm$ 2	68 $\pm$ 1	60 $\pm$ 1

Droplet shape is another factor that differed between the different emulsions (Figure 1 and Figure S11). A-emulsion droplets tended to coalesce during the emulsification process, resulting in mostly non-spherical droplets due to their high surface coverage (Figure 1A). N- and C-emulsions droplets were mostly spherical (Figure 1C). A/N-emulsions were slightly deformed with the presence of some non-spherical droplets (Figure 1B), and C/N-emulsions droplets were spherical. The shape of the A/C-emulsion droplets prepared at 24 000 rpm was slightly non-spherical, but the droplets prepared at 6 500 rpm were spherical. This is due to the rapid adsorption rate of the particles and the high surface coverage of the droplets prepared at 6 500 rpm. These differences have been previously investigated and reported in detail [19].

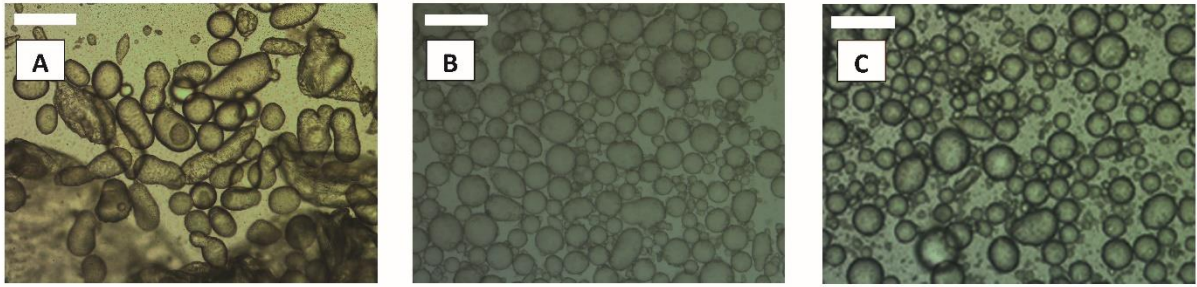


**Figure 1.** Optical microscopy pictures of Pickering emulsions with 43 mg of particles per cm<sup>3</sup> of oil. From left to right, A-emulsion (non-spherical), A/N-emulsion (slightly non-spherical), N-emulsion (mostly spherical). The white scale bar is 200  $\mu$ m.

### 3.2. Rheological properties and stability

#### **3.2.1. Viscoelasticity of the emulsions**

The viscoelastic properties of the prepared emulsions were studied via oscillatory rheological measurements at 25 °C. As shown in [Figure 2](#) for A-, N- and C-emulsions, the storage ( $G'$ ) and loss ( $G''$ ) moduli were relatively independent of the angular frequency  $\omega$  over a wide range. This was observed irrespective of the particle concentration or the stirring rate used for emulsification. The same behavior was obtained for DCPs (results not shown). Such rheological properties are typical of Pickering emulsions with a high oil volume fraction and are characteristic of highly flocculated elastic structures [30–32]. Moreover,  $G''/G' = \tan(\delta)$  remained constant and lower than 0.15 for all emulsions, indicating strongly elastic (solid-like) behavior.

These results indicated physically stable Pickering emulsions that behave as strong gels [33]. The present oscillatory measurements were carried out in the usual linear regime where the small applied deformation was such that  $G'$  did not depend on the strain. The stress was also low, lower than the yield stress of the gel. Accordingly, the emulsion structure was retained during these measurements. This is the case of emulsion droplets in the gelled creamed layer. Viscosity measurements are of poor relevance in the context of the present study because they require that the stress is larger than the yield for the sample can flow. Flowing causes the gel destructuring, that is, the modification of the emulsion structure that does not occur in the quiescent creamed layer. As one of the main objectives of this study was to better understand the structure of the Pickering emulsions, i.e. the deformability of the droplets, only oscillatory stress measurements were considered as the most relevant experiments.

Therefore,  $G'$  was used as the relevant parameter to describe the rheological properties of the emulsions in the remainder of the study. The shear viscosity behavior of all emulsions was nevertheless measured ([Figure S12](#)) and no significant differences were found between them.

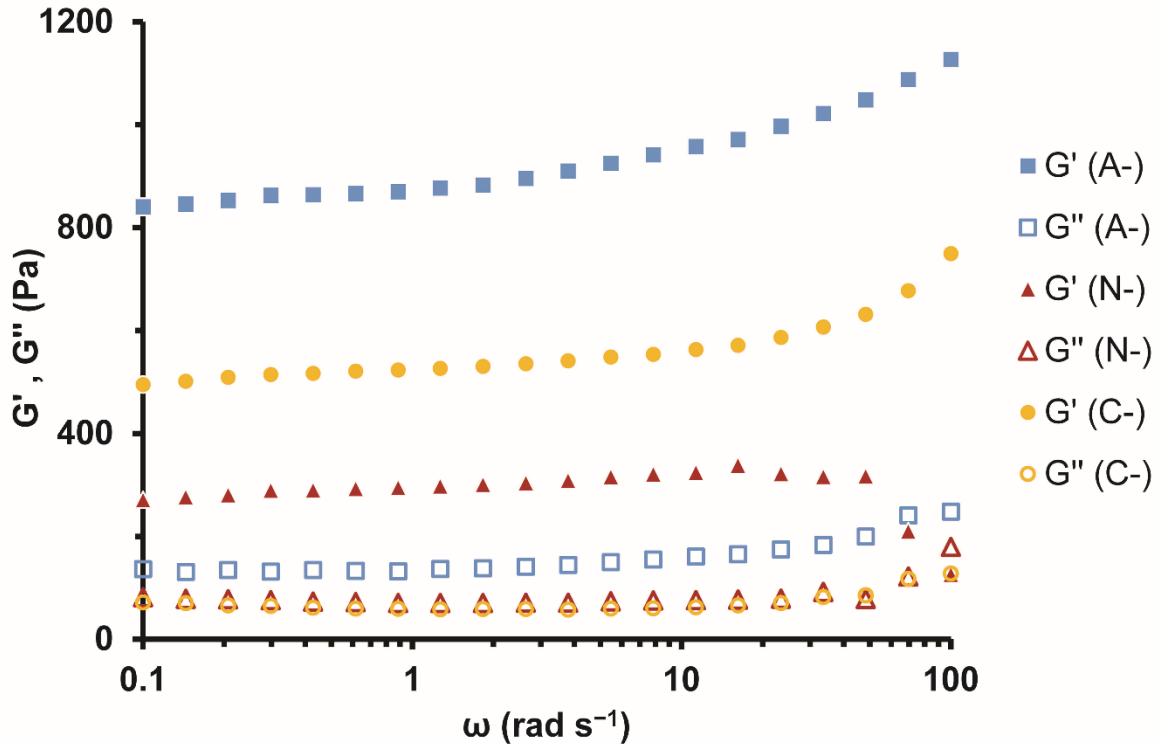


**Figure 2.** Storage ( $G'$ ) and loss ( $G''$ ) moduli measured at 25 °C as a function of the angular frequency  $\omega$  for A-, N-, and C-emulsions prepared at 24 000 rpm with 32 mg of particles per  $\text{cm}^3$  of oil.

Figure 3 displays the evolution of  $G'$  for all the emulsion types prepared at 6 500 rpm at three different particle concentrations.  $G'$  varied between 74 and 911 Pa. Considering the experimental error determined from triplicate measurements, no significant variation of  $G'$  against the particle concentration was observed for a given emulsion type. Similar results were obtained for emulsions prepared at 24 000 rpm. These results suggested that the rheological properties of the emulsions were not due to the interactions between the particles in the continuous phase. Thus, the viscosity of 2 wt% suspensions of the 3 types of particles (results not shown) showed that particle aggregation did not occur because the viscosity was independent of the shear rate (Newtonian behavior) and not significantly different from that of pure water ( $\sim 1.2 \text{ mPa}\cdot\text{s}$ ) [12,14]. These experiments on particle suspensions (no oil) were representing the worst case where all particles were dispersed in the continuous phase; indeed, 2 wt% is the ratio of the mass of particles to the mass of water in the creamed emulsion prepared at a particle concentration of  $40 \text{ mg}\cdot\text{cm}^{-3}$ . The actual concentration of particles in the aqueous phase was much lower as almost all particles were adsorbed at the o/w interface (no particles were detected in the aqueous phase of the emulsions [19]).

As explained in the introduction, the elastocapillary number  $Ca_G$  is used to assess if the droplets are deformed under oscillatory stress. Using these results, the elastocapillary number was determined for all emulsions (Eq. 2). The measured water/oil interfacial tension was  $31 \text{ mN}\cdot\text{m}^{-1}$ . The value of  $Ca_G$  was between 0.2 and 4.1 for all emulsions. As  $Ca_G \approx 1$ , the

droplets are likely to deform during the experiment [12,14,15]. The deformation of C-emulsion droplets in a flow was observed by subjecting them to a slow flow under microscopic observation (see VideoSI3.mp4).

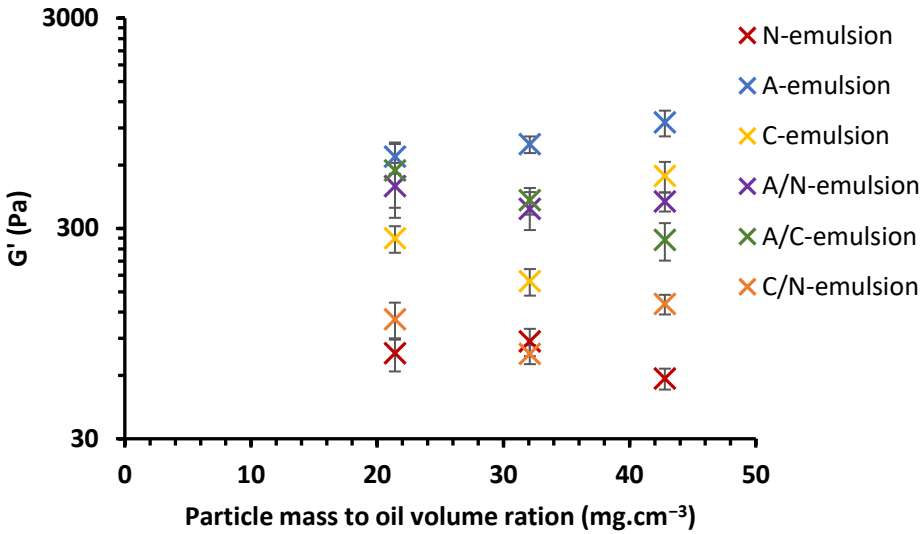


**Figure 3.**  $G'$  as a function of the (particle mass to oil volume) ratio for the different emulsion types prepared at 6 500 rpm. The Y-axis is shown in log scale for better readability. Results are given as Mean  $\pm$  SEM ( $n = 3$ ).

Figure 4 shows the mean  $G'$  values measured for the different emulsions at 6 500 and 24 000 rpm for the three different particle concentrations.  $G'$  was lower for the emulsions prepared at 6 500 rpm, for a same type of emulsion. The difference was significant for N- and A/C-emulsions. It was below significance for other emulsions; only a trend could be devised. This result was likely due to the lower particle coverage when preparing the N- and A/C-emulsions at 6 500 rpm (Table 2). A more detailed discussion is given in section 4.

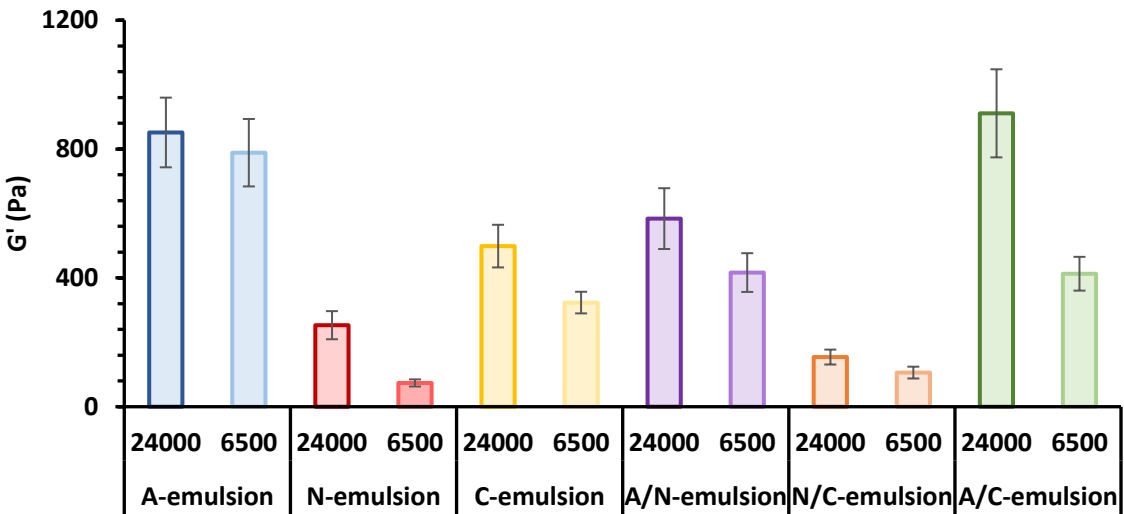


**Figure 4.**  $G'$  values measured for the different emulsions. Results are represented as Mean  $\pm$  SEM ( $n = 3$ ).

The particle surface charge, whether they are alone or mixed, and the stirring rate during emulsification influence both droplet coverage and morphology [19]. It is difficult to compare the rheological behavior of the different emulsions taken all together because this is a multi-parametric problem; emulsion droplets do not have the same size and coverage. Therefore, comparisons were only made between emulsions with similar coverages, resulting in three coarse categories of emulsions: high  $G'$ , intermediate  $G'$  and low  $G'$  (Table 3).

The A-emulsions have a very high coverage similar to that of the A/N(6 500)-emulsion ( $\approx 90\%$ ). However, the A/N(6 500)-emulsion showed a lower  $G'$  (resp. 789 Pa and 417 Pa). The same observation applies to A/C(24 000)- and N(24 000)-emulsion (coverage  $\approx 70\%$ ). The A/C(6 500)- and C(24 000)-emulsions had a similar coverage ( $\approx 60\%$ ) and a similar  $G'$ . This was also the case for C(6 500)- and N(24 000)-emulsions (coverage  $\approx 67\%$ ), and for N(24 000) and N/C(6 500)-emulsions (coverage  $\approx 72\%$ ). Table 3 summarizes these observations and classifies the emulsions into three categories according to a sequence of  $G'$  values: A-emulsions  $>$  A/C(24 000)- and A/N- and emulsions  $>$  N-, C-, A/C(6 500)- and N/C- emulsions.

Table 3 shows that the differences in  $G'$  between two emulsions with similar droplet coverage are mainly due to the droplet morphology rather than to the surface charges of the droplets. The presence of non-spherical droplets tends to increase the storage modulus. This result is developed in the discussion section.

**Table 3.** Categorization of the different natures of emulsions based on the  $G'$  modulus and droplet morphology.

	High $G'$	Intermediate $G'$	Low $G'$
Mostly non-spherical droplets	A-emulsions	/	/
Presence of non-spherical droplets	/	A/N-emulsions A/C(24 000)-emulsions	/
Spherical droplets	/	/	N-emulsions C-emulsions A/C(6 500)-emulsions N/C-emulsions

### 3.2.2. Thermal ageing test

After emulsification, the emulsions were transferred into small vials in order to easily detect the possible appearance of an oil layer on top of the samples indicating emulsion destabilization. Only A-emulsions showed a layer of pure released oil above the creamed emulsion layer after two months storage at 45 °C. After three months storage, the emulsions were classified into three classes based on visual characterization: no destabilization (Class 1, Figure 5A), presence of oil globules (Class 2, Figure 5B) or of an oil layer (Class 3, Figure 5C) on top of the samples. These characteristics allow a good evaluation of coalescence intensity in the emulsions. The results are given in Table 4.

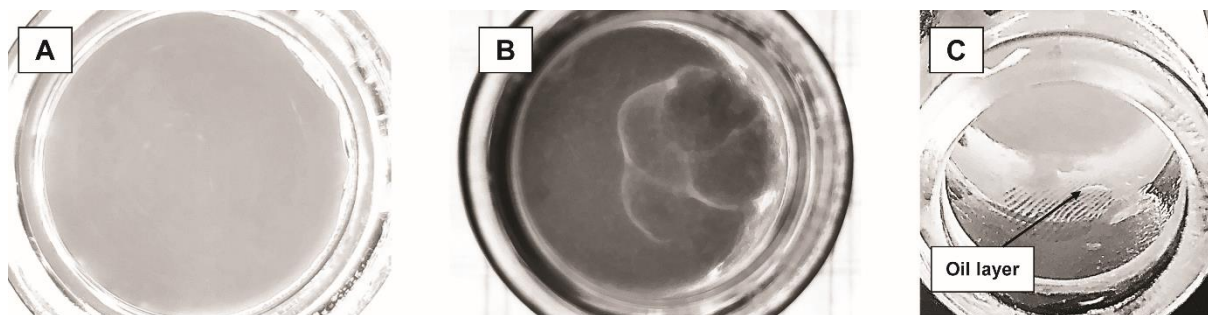


**Figure 5.** The three types of destabilization observed. A: No or very slight signs of destabilization from C-emulsion. B: Presence of oil globules at the surface of A/N-emulsion. C: Presence of a supernatant oil layer from A-emulsion.

A-emulsions were the most unstable, while C-emulsions showed no signs of destabilization. N-emulsions only exhibited a few oil globules at their surface. In N/C-emulsions, oil globules were present when prepared with  $21 \text{ mg}\cdot\text{cm}^{-3}$  of particles, but not with  $42 \text{ mg}\cdot\text{cm}^{-3}$ . For A/N-emulsions, an oil layer was present at  $21 \text{ mg}\cdot\text{cm}^{-3}$  of particles, but only oil globules at  $42 \text{ mg}\cdot\text{cm}^{-3}$ . Only a slight destabilization occurred in the A/C-emulsions.

For all the emulsions in which destabilization occurred (N-, A-, A/N- and N/C-emulsions), oil release was faster at low particle concentration ( $21 \text{ mg}\cdot\text{cm}^{-3}$ ). Moreover, no significant differences were noticed between emulsions prepared at 6 500 rpm and 24 000 rpm whatever the particles used as emulsifier.

A stability sequence can be derived from these observations: C-, A/C- and N/C( $43 \text{ mg}\cdot\text{cm}^{-3}$ )-emulsions > N-, N/C( $21 \text{ mg}\cdot\text{cm}^{-3}$ )- and A/N( $43 \text{ mg}\cdot\text{cm}^{-3}$ )-emulsions > A- and A/N( $21 \text{ mg}\cdot\text{cm}^{-3}$ )-emulsions (Table 4).

**Table 4.** Stability results after 3 months storage of the emulsions at  $45 \text{ }^\circ\text{C}$  (thermal ageing test). No significant differences were observed between emulsions prepared at 6 500 rpm and 24 000 rpm.

No visible signs of destabilization	Presence of several globules at the top of the emulsion	Presence of an oil layer at the top of the emulsion
C-emulsions	N-emulsions	A-emulsions
A/C-emulsions	N/C-emulsions ( $21 \text{ mg}\cdot\text{cm}^{-3}$ )	A/N-emulsions ( $21 \text{ mg}\cdot\text{cm}^{-3}$ )
N/C-emulsions ( $43 \text{ mg}\cdot\text{cm}^{-3}$ )	A/N-emulsions ( $43 \text{ mg}\cdot\text{cm}^{-3}$ )	

### 3.2.3. Forced coalescence experiments

To perform forced coalescence tests, the emulsions were centrifuged at 4000 rpm for 1 h and the time evolution of the transmitted light was measured over the full height of the samples. Analysis of the transmission profiles gives the evolution of the emulsion with the possible appearance of a clear supernatant oil layer and a clear subnatant water layer (Figure 6). At the end of the experiment, the ratio of the height of the released phase (oil in this case) to the initial height of the emulsion sample was taken as the separation index. This characterization is the one commonly used and proposed by the SEPView® software of the LUMiSizer®



instrument [34,35]. The lower the separation index, the more stable the emulsion against forced coalescence. The separation index decreased with the droplet size for all types of emulsions (Figure 7).

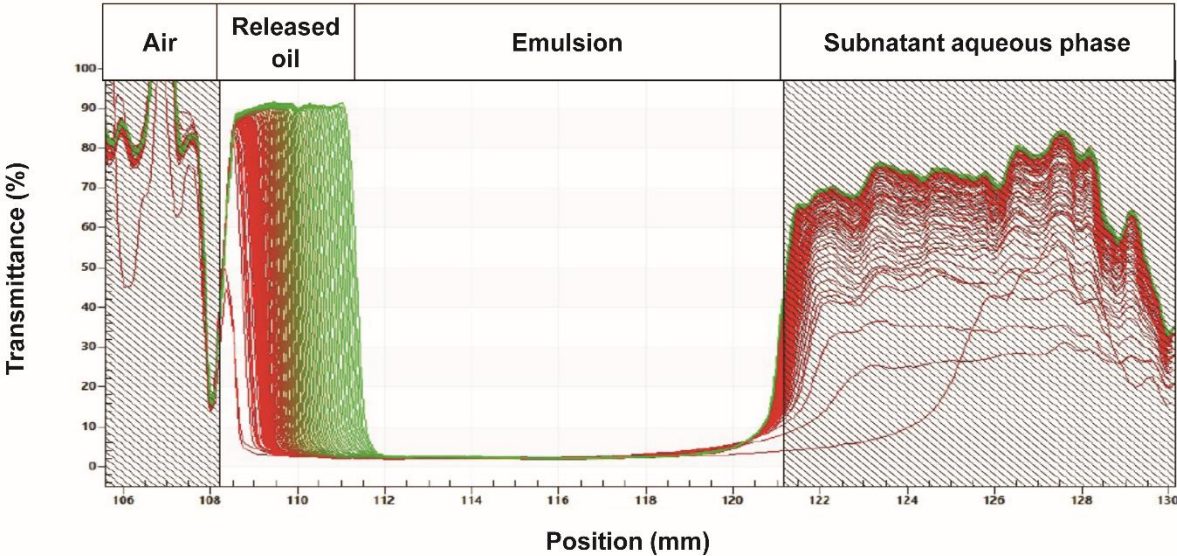


**Figure 6.** Time evolution of the transmission profiles as a function of the height in an N-emulsion sample during centrifugation at 4000 rpm for 1 h. Red lines represent the profiles at the start of the experiment and the green ones at the end. The creaming process was characterized by the appearance of an aqueous subnatant phase. Emulsion destabilization was characterized by the appearance of an oil supernatant phase.

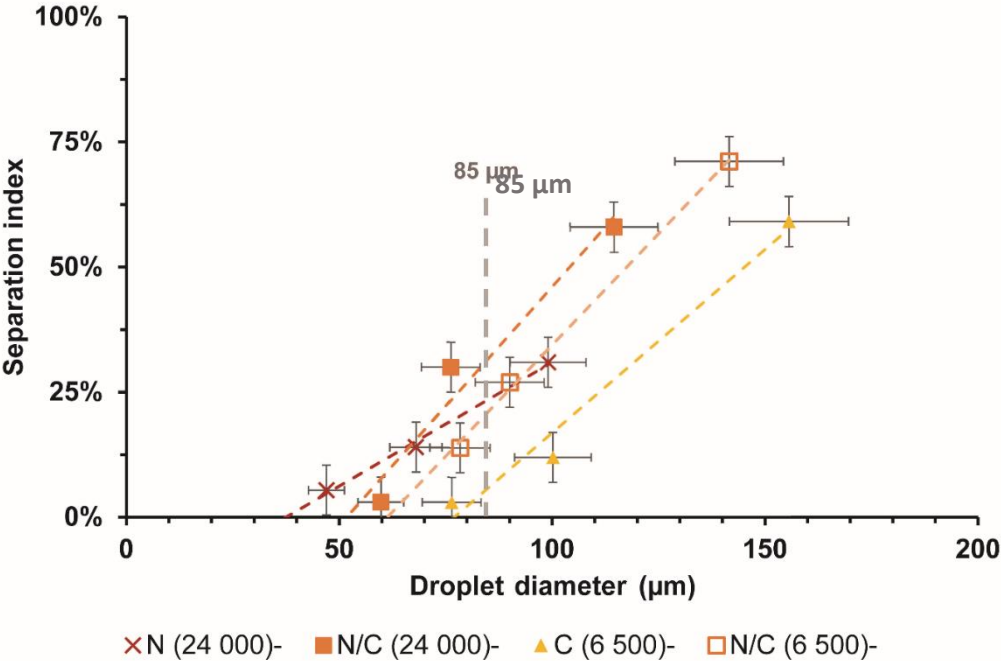


**Figure 7.** Separation index of 4 different emulsions as a function of their droplet diameters. Three concentrations were used for each emulsion type (21, 32 and 43 mg of particles per cm<sup>3</sup> of oil). The separation index at 85 μm droplet diameter,  $S_{85}$ , was obtained by linear extrapolation.

To compare the separation index of the whole set of emulsions with different droplet sizes, the separation index for a droplet diameter of 85  $\mu\text{m}$  ( $S_{85}$ ) was linearly extrapolated (Figure 8). The lower was the  $S_{85}$ , the more resistant the emulsion was to forced coalescence. Emulsions prepared at 6 500 rpm were always more resistant than those prepared at 24 000 rpm, except for A-emulsions where the emulsification process did not alter the properties.

A-emulsions ( $S_{85} > 40\%$ ) and C-emulsions ( $S_{85} < 10\%$ ) were respectively the least and the most resistant emulsions. N- and N/C- emulsions had intermediate  $S_{85}$  values  $\sim 20\text{--}30\%$ . A/N-emulsions showed low resistance to forced coalescence and their corresponding  $S_{85}$  values  $\sim 30\text{--}35\%$  were between those of A- and N-emulsions. For A/C-emulsions, the  $S_{85}$  value for the emulsions prepared at 24 000 rpm was similar to A/N-ones  $\sim 35\%$ , but a very low  $S_{85}$  value  $\sim 10\%$  was obtained at 6 500 rpm. These results were consistent with the thermal ageing tests. Table 5 shows the droplet diameters of the emulsions after the centrifugation tests. In all cases, the post-centrifugation diameters were smaller than the initial diameters.

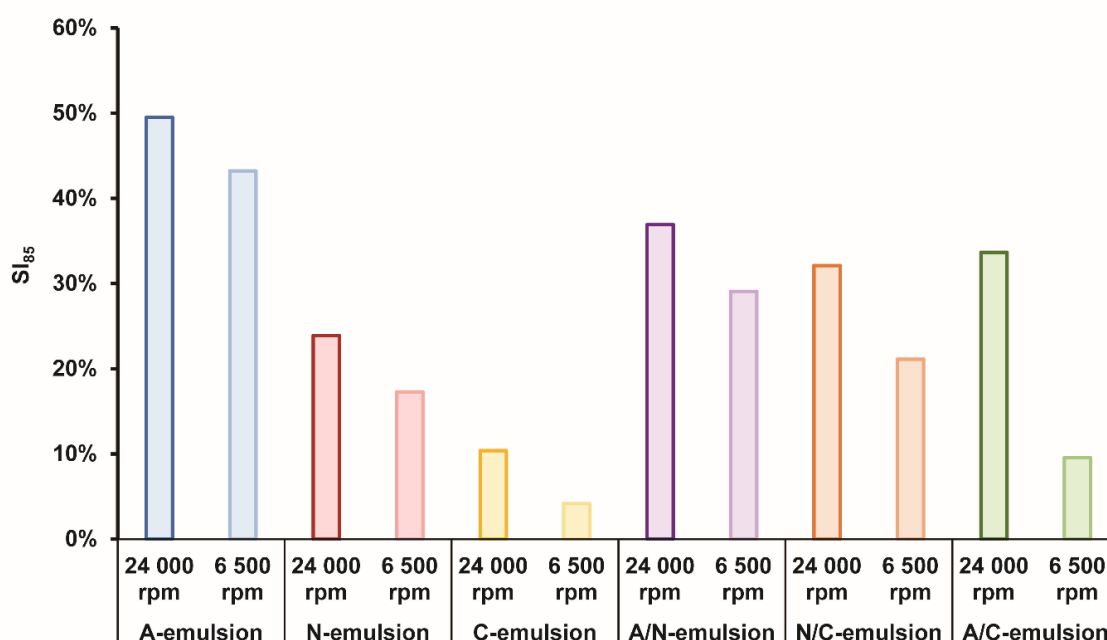


**Figure 8.** Stability against forced coalescence by centrifuge of the different emulsions. The stability is represented by  $S_{85}$ ; low  $S_{85}$  indicates more stable emulsion.

**Table 5.** Comparison of the droplets diameter before and after forced coalescence test. All the emulsions presented were prepared at a mass of particles over oil volume ratio of 21  $\text{mg}\cdot\text{cm}^{-3}$ .

Emulsion type	Stirring rate (rpm)	Initial droplet diameter ( $\mu\text{m}$ )	Post-centrifugation droplet diameter ( $\mu\text{m}$ )	Variation
A-		195	147	-25%
N/C-	24 000	114	90	-21%
A/C-		161	142	-12%
A-		196	170	-13%
N/C-	6 500	142	89	-37%
A/C-		140	120	-14%

#### 4. General discussion

The factors influencing the rheological behavior of Pickering emulsions are not fully understood so far. For example, depending on the system studied, the concentration of particles used as emulsifiers either increases the viscous response of an emulsion [9,31], or, as in the present study, has no significant effect at high particle concentrations [4,30]. Increasing the concentration of salt in the dispersed phase either decreases [9], has no effect [11], or increases the viscosity of the emulsion [7]. As a whole, some important parameters influencing the rheology of Pickering emulsions are still unknown. In order to further investigate the response of these systems due to droplet deformation, interfacial rheology experiments have shown that increasing the coverage of the oil-water interface with the emulsifier tends to stiffen it [36,37]. The effect of the coverage on the bulk rheology of emulsions has not been investigated yet.

On the other hand, the factors influencing the stability of Pickering emulsions against coalescence are better known and most experimental results are consistent. High coverage increases emulsion stability [38], and emulsions with smaller droplets are more stable [39]. Charged emulsifiers prevent coalescence by limiting the flocculation [40,41] although flocculation without coalescence has also been observed [42]. It is worth noting that the comparison between coalescence under thermal ageing and centrifuge-induced coalescence of Pickering emulsions has not been addressed so far.

Finally, as mentioned in the introduction, the relationship between rheology and stability has been studied in order to better understand both these phenomena and to be able to predict one from the other. The present study has provided new insight into the role of two poorly studied parameters: the coverage and the morphology of the droplets.

#### Rheological behavior

As mentioned before, no particles in suspension were detected in the bulk of the continuous phase. Moreover, the capillary number calculations showed that the droplets are highly deformable. Therefore, the rheological properties of the emulsions is likely to be due to the droplet deformation rather than to the formation of a 3D-network of particles bound together by attractive interactions. The results of this study therefore provide information on the influence of droplet surface coverage and morphology on the rheological properties of emulsions. Both parameters, droplets coverage and morphology, are highly linked to the surface charge of the particles [19].

As can be seen in Table 2, decreasing the mixing speed from 24 000 rpm down to 6 500 rpm increased the coverage of the droplet surface by the particles, except for the A-emulsion droplets, which had similar coverage, and the A/C emulsions whose droplet coverage decreased. And, as already mentioned, the general trend is that  $G'$  was lower for the emulsions prepared at 6 500 rpm. The increase in coverage could therefore partly explain the lower  $G'$  observed for the emulsions made at 6 500 rpm compared to those made at 24 000 rpm.

In the literature, the comparison of the rheological behavior of suspensions of hard and soft spheres have shown that softer spheres have higher loss and storage moduli because they can deform and create more contact area between them. More contact area results in more cohesive interactions, leading to a higher suspension viscosity [43,44]. Moreover, droplet deformation should result in a high energy storage because the droplets return back to their original shape when the stress is stopped. Higher droplet coverage results in a stiffer interface and the droplet behavior should be closer to that of hard spheres characterized by low  $G'$  and viscosity. Decreasing the droplet surface coverage would increase both the area of contact between droplets and their deformability, resulting in an increase in the storage modulus. The deformation of C-emulsion droplets in a flow was observed by subjecting them to a slow flow under microscopic observation (see [VideoSI3.mp4](#)).

Next, it is difficult to compare the influence of particle charge on the  $G'$  of the emulsions because the resulting droplets did not have the same surface coverage. Emulsions with similar coverage were compared and [Table 3](#) summarizes these comparisons.

As observed in [Table 3](#), the morphology of the emulsion droplets was sufficient to explain the storage moduli of the emulsions: more spherical droplets result in higher  $G'$ . This could be explained by the fact that, *i*) non-sphericity increases the contact area between droplets, leading to a more rigid 3D-network and *ii*) the alignment of emulsion droplets under oscillatory shear stress could be promoted for spherical droplets rather than for non-spherical and heterogeneous ones. Better alignment of the droplets would diminish the storage modulus of the emulsion.

### **Emulsion stability**

It is worth noting that, in the case of this study, Ostwald ripening was a negligible phenomenon in all experiments. Indeed, this phenomenon is negligible when the two phases are highly immiscible. Moreover, the ripening rate diminishes with the droplet size, becoming almost null for droplet diameters larger than 1  $\mu\text{m}$  [45]. Thus, only the coalescence was considered as a destabilization mechanism influencing the droplet diameter. A good illustration of centrifugation as a tool for assessing emulsion stability is given by Tcholakova *et al.* [24] who studied the coalescence of  $\beta$ -lactoglobulin-stabilized o/w emulsions under a compressive force caused by centrifugation. Such forced coalescence involves two distinct phenomena. When an emulsion is placed in a centrifuge, two phenomena occur simultaneously: droplet-droplet coalescence and coalescence of droplets with the supernatant oil layer. The second mechanism is probably the most important. Indeed, the measured median size of the emulsion droplets decreased after the forced coalescence experiments ([Table 5](#)). Of course, the static pressure generated by centrifugation cannot cause droplet fragmentation. Therefore, the decrease in size is due to the coalescence of the largest droplets with the supernatant oil layer, leaving the smallest droplets in the emulsion. Indeed, creaming is faster for the largest droplets that reach first and accumulate on top of the creamed emulsion layer in contact with the forming supernatant layer of released oil. Moreover, larger droplets are less resistant to the centrifuge pressure because their internal pressure is lower [24].

It is worth noting that the stability results obtained with the forced coalescence test and the thermal ageing experiments were consistent. The similarity of results for forced coalescence by centrifuge and thermal ageing has already been noticed on classical emulsions [46], and forced coalescence is recognized as a way to measure the stability of cosmetic products (ISO/TR 18811). A major difference is the effect of droplet coverage on the emulsion stability that was not observable in thermal ageing experiments. However, the influence of the particle charge on the emulsion stability was more important than changing the stirring rate for emulsion preparation. In the case of Pickering emulsions that resist coalescence, a thermal ageing test with visual inspection was not precise enough to accurately discriminate the origin of their stabilization.

When comparing MTP emulsions, A-emulsions were the least stable, and N-emulsions were less stable than C-ones. The destabilization of A-emulsions could be due to the presence of non-spherical droplets. Indeed, coalescence is due to the merging of two colliding droplets. For a given individual droplet volume, the non-spherical shape results in a higher surface area. Then the probability of collision between droplets is also higher. The oriented wedge theory states that two droplet surfaces flatten when they are coming into contact, and a channel can nucleate and grow, leading to droplet coalescence [47]. The energy required to flatten the interface is proportional to the curvature of the droplets at the point of contact [48]. A less curved interface could then favor the coalescence between two droplets. For the same reason, as observed in both types of stability experiments, small droplets would be more stable because of their high curvature value.

C- and N-emulsions both have spherical droplets but the C-emulsions droplets were more resistant to coalescence. One explanation could be that the spherical and positively charged C-emulsions droplets strongly repel each other. The barrier against coagulation is higher than for N-emulsions, and therefore coalescence should be slowed down [40,41]. In forced coalescence, the pressure exerted on the oil droplets causes the water film between the oil layer and the droplets to drain, resulting in coalescence at the droplet-oil layer interface [24,49]. Once again, the difference of stability could be explained by the same mechanisms: i) spherical droplets with high internal pressure that would hardly be drained and ii) cationic particles that can easily adsorb at the oil/water interface [19,50]. The interface of the droplets and the released oil layer at the top of an emulsion sample would both be positively charged and have a tendency to repel each other, limiting the draining effect. It is interesting to note that, even if the A-emulsions droplets are charged, this phenomenon seems to be far less decisive for emulsion stability than the effect of the morphology of the droplets.

A/N-emulsions showed an intermediate behavior between their corresponding MTPs. Given their moderate sphericity and charge, the above arguments explain their intermediate stability. The similar stabilities of N/C- and N-emulsions can be explained by their low surface charges that are not sufficient to significantly prevent coalescence.

Interestingly, A/C-emulsions were more stable than expected. A/C-emulsions prepared at 24 000 rpm had non-spherical and neutral droplets with a lower droplet surface coverage than A/N-emulsions. They should therefore destabilize. A/C-emulsions prepared at 6 500 rpm with

spherical but neutral droplets should show medium destabilization. These results could be due to the formation of a 2D-network due to interactions between the oppositely charged c- and a-PMMA particles at the droplet surface, which would stiffen it. Indeed, Thijssen *et al.* [36] showed that the interfacial viscosity of a particle-covered interface was influenced by their interfacial organization (aggregated or organized as a colloidal crystal). If the droplet interface were more rigid, the pressure required to deform it and cause the droplets to coalesce would also be higher.

Finally, no strong correlation was found between rheology and stability measurements. Even though the stiffness, coverage or morphology of the emulsion droplets strongly influenced both the stability and the viscoelasticity of the emulsions, many differences were observed. For example, the particle surface charges influenced the emulsion stability, but not their viscoelasticity properties, making it difficult to predict their stability from rheology experiments alone, or vice versa.

## 5. Conclusion and prospects

In this article, Pickering emulsions stabilized with anionic, neutral and cationic PMMA-like particles were prepared. The rheological properties and the stability of the concentrated emulsions were studied to analyze the effect of the particle charge. Subsequently, 50/50 binary mixtures of these particles were used as emulsifiers to prepare emulsions whose stability and rheological properties were studied.

The viscoelastic behavior of the emulsions was mostly elastic ( $G' \gg G''$ ). The results suggest that  $G'$  was mainly related to the droplet shape and deformability. The morphology of the droplets had a strong influence on both their rheological behavior and stability. The presence of non-spherical droplets increased the viscosity of the emulsions while decreasing their resistance to both thermal ageing and forced coalescence.

The particles coverage of the droplets was also shown to be a relevant parameter. Higher coverage resulted in a lower storage modulus but a better stability against forced coalescence. That is of particular interest for practical applications because the coverage of an emulsion can be easily manipulated [19]. It was also shown that forced coalescence by centrifugation is a relevant way to study the accelerated destabilization of Pickering emulsions stabilized by polymeric particles. However, no obvious correlations were found between rheological properties and stability of Pickering emulsions although these two properties depend on the same parameters.

Finally, the emulsions stabilized by a binary mixture of anionic and cationic particles showed high stability despite the presence of either non-spherical droplets or low droplet surface coverage. One reason could be the formation of a 2D rigid network at the surface of the droplets due to the attractive interactions between anionic and cationic particles. Interfacial rheology experiments could be a way to further investigate and better understand the role of interfacial stiffness in the stability of these Pickering emulsions.

## References

- [1] Y. Chevalier, M.-A. Bolzinger, Emulsions stabilized with solid nanoparticles: Pickering emulsions. *Colloids Surfaces A: Physicochem Eng Aspects*, 439 (2013) 23–34, doi: [10.1016/j.colsurfa.2013.02.054](https://doi.org/10.1016/j.colsurfa.2013.02.054).
- [2] J. Frelichowska, M.-A. Bolzinger, Y. Chevalier, Pickering emulsions with bare silica. *Colloids Surfaces A: Physicochem Eng Aspects*, 343 (2009) 70–74, doi: [10.1016/j.colsurfa.2009.01.031](https://doi.org/10.1016/j.colsurfa.2009.01.031).
- [3] J. Chen, R. Vogel, S. Werner, G. Heinrich, D. Clause, V. Dutschk, Influence of the particle type on the rheological behavior of Pickering emulsions. *Colloids Surfaces A: Physicochem Eng Aspects*, 382 (2011) 238–245, doi: [10.1016/j.colsurfa.2011.02.003](https://doi.org/10.1016/j.colsurfa.2011.02.003).
- [4] C. Griffith, H. Daigle, Manipulation of Pickering emulsion rheology using hydrophilically modified silica nanoparticles in brine. *J Colloid Interface Sci*, 509 (2018) 132–139, doi: [10.1016/j.jcis.2017.08.100](https://doi.org/10.1016/j.jcis.2017.08.100).
- [5] E. Dłużewska, A. Stobiecka, M. Maszewska, Effect of oil phase concentration on rheological properties and stability of beverage emulsions. *Acta Sci Pol Technol Aliment*, 5 (2006) 147–156, [https://www.food.actapol.net/volume5/issue2/14\\_2\\_2006.pdf](https://www.food.actapol.net/volume5/issue2/14_2_2006.pdf).
- [6] C.P. Whitby, L. Lotte, C. Lang, Structure of concentrated oil-in-water Pickering emulsions. *Soft Matter*, 8 (2012) 7784–7789, doi: [10.1039/c2sm26014j](https://doi.org/10.1039/c2sm26014j).
- [7] T.S. Horozov, B.P. Binks, T. Gottschalk-Gaudig, Effect of electrolyte in silicone oil-in-water emulsions stabilised by fumed silica particles. *Phys Chem Chem Phys*, 9 (2007) 6398–6404, doi: [10.1039/b709807n](https://doi.org/10.1039/b709807n).
- [8] L. Yu, S. Li, L.P. Stubbs, H.C. Lau, Rheological investigation of clay-stabilized oil-in-water Pickering emulsions for potential reservoir applications. *J Petr Sci Eng*, 204 (2021) 108722, doi: [10.1016/j.petrol.2021.108722](https://doi.org/10.1016/j.petrol.2021.108722).
- [9] J. Xiao, X. Wang, A.J. Perez Gonzalez, Q. Huang, Kafirin nanoparticles-stabilized Pickering emulsions: Microstructure and rheological behavior. *Food Hydrocolloids*, 54 (2016) 30–39, doi: [10.1016/j.foodhyd.2015.09.008](https://doi.org/10.1016/j.foodhyd.2015.09.008).
- [10] C. Miao, M.-N. Mirvakili, W.Y. Hamad, A rheological investigation of oil-in-water Pickering emulsions stabilized by cellulose nanocrystals. *J Colloid Interface Sci*, 608 (2022) 2820–2829, doi: [10.1016/j.jcis.2021.11.010](https://doi.org/10.1016/j.jcis.2021.11.010).
- [11] W.J. Frith, R. Pichot, M. Kirkland, B. Wolf, Formation, stability, and rheology of particle stabilized emulsions: Influence of multivalent cations. *Ind Eng Chem Res*, 47 (2008) 6434–6444, doi: [10.1021/ie071629e](https://doi.org/10.1021/ie071629e).
- [12] H. Katepalli, V.T. John, A. Tripathi, A. Bose, Microstructure and rheology of particle stabilized emulsions: Effects of particle shape and inter-particle interactions. *J Colloid Interface Sci*, 485 (2017) 11–17, doi: [10.1016/j.jcis.2016.09.015](https://doi.org/10.1016/j.jcis.2016.09.015).
- [13] C.P. Whitby, F.E. Fischer, D. Fornasiero, J. Ralston, Shear-induced coalescence of oil-in-water Pickering emulsions. *J Colloid Interface Sci*, 361 (2011) 170–177, doi: [10.1016/j.jcis.2011.05.046](https://doi.org/10.1016/j.jcis.2011.05.046).
- [14] B.P. Binks, J.H. Clint, C.P. Whitby, Rheological behavior of water-in-oil emulsions stabilized by hydrophobic bentonite particles. *Langmuir*, 21 (2005) 5307–5316, doi: [10.1021/la050255w](https://doi.org/10.1021/la050255w).
- [15] M.-D. Lacasse, G.S. Grest, D. Levine, T.G. Mason, D.A. Weitz, Model for the elasticity of compressed emulsions. *Phys Rev Lett*, 76 (1996) 3448–3451, doi: [10.1103/PhysRevLett.76.3448](https://doi.org/10.1103/PhysRevLett.76.3448).

- [16] C. Py, J. Rouvière, P. Loll, M.C. Taelman, Th.F. Tadros, Investigation of multiple emulsion stability using rheological measurements. *Colloids Surfaces A: Physicochem Eng Aspects*, 91 (1994) 215–225, doi: [10.1016/0927-7757\(94\)02918-0](https://doi.org/10.1016/0927-7757(94)02918-0).
- [17] Z.H. Tekin, E. Avci, S. Karasu, O.S. Toker, Rapid determination of emulsion stability by rheology-based thermal loop test. *LWT*, 122 (2020) 109037, doi: [10.1016/j.lwt.2020.109037](https://doi.org/10.1016/j.lwt.2020.109037).
- [18] T. Tadros, Application of rheology for assessment and prediction of the long-term physical stability of emulsions. *Adv Colloid Interface Sci*, 108–109 (2004) 227–258, doi: [10.1016/j.cis.2003.10.025](https://doi.org/10.1016/j.cis.2003.10.025).
- [19] M. Benyaya, M.-A. Bolzinger, Y. Chevalier, S. Ensenat, C. Bordes, Pickering emulsions stabilized with differently charged particles. *Soft Matter*, 19 (2023) 4780–4793, doi: [10.1039/D3SM00305A](https://doi.org/10.1039/D3SM00305A).
- [20] M. Benyaya, M.-A. Bolzinger, Y. Chevalier, C. Bordes, Formulation of polymeric particles with controlled charges by alkaline tempering. *Polymer*, 272 (2023) 125838, doi: [10.1016/j.polymer.2023.125838](https://doi.org/10.1016/j.polymer.2023.125838).
- [21] H. Masmoudi, Y.L. Dréau, P. Piccerelle, J. Kister, The evaluation of cosmetic and pharmaceutical emulsions aging process using classical techniques and a new method: FTIR. *Int J Pharm*, 289 (2005) 117–131, doi: [10.1016/j.ijpharm.2004.10.020](https://doi.org/10.1016/j.ijpharm.2004.10.020).
- [22] G. Chansiri, R.T. Lyons, M.V. Patel, S.L. Hem, Effect of surface charge on the stability of oil/water emulsions during steam sterilization. *J Pharm Sci*, 88 (1999) 454–458, doi: [10.1021/js980293i](https://doi.org/10.1021/js980293i).
- [23] J. Liu, J. Guo, H. Zhang, Y. Liao, S. Liu, D. Cheng, T. Zhang, H. Xiao, Z. Du, The fabrication, characterization, and application of chitosan–NaOH modified casein nanoparticles and their stabilized long-term stable high internal phase Pickering emulsions. *Food Funct*, 13 (2022) 1408–1420, doi: [10.1039/D1FO02202D](https://doi.org/10.1039/D1FO02202D).
- [24] S. Tcholakova, N.D. Denkov, I.B. Ivanov, B. Campbell, Coalescence in  $\beta$ -lactoglobulin-stabilized Emulsions: Effects of protein adsorption and drop size. *Langmuir*, 18 (2002) 8960–8971, doi: [10.1021/la0258188](https://doi.org/10.1021/la0258188).
- [25] F. Goodarzi, S. Zendejboudi, A comprehensive review on emulsions and emulsion stability in chemical and energy industries. *Can J Chem Eng*, 97 (2019) 281–309, doi: [10.1002/cice.23336](https://doi.org/10.1002/cice.23336).
- [26] D.J. McClements, Critical review of techniques and methodologies for characterization of emulsion stability. *Crit Rev Food Sci Nutr*, 47 (2007) 611–649, doi: [10.1080/10408390701289292](https://doi.org/10.1080/10408390701289292).
- [27] H.M. Princen, Osmotic pressure of foams and highly concentrated emulsions. I. Theoretical considerations. *Langmuir*, 2 (1986) 519–524, doi: [10.1021/la00070a023](https://doi.org/10.1021/la00070a023).
- [28] J. Frelichowska, M.-A. Bolzinger, Y. Chevalier, Effects of solid particle content on properties of o/w Pickering emulsions. *J Colloid Interface Sci*, 351 (2010) 348–356, doi: [10.1016/j.jcis.2010.08.019](https://doi.org/10.1016/j.jcis.2010.08.019).
- [29] R. Pal, Effect of droplet size on the rheology of emulsions. *AIChE J*, 42 (1996) 3181–3190, doi: [10.1002/aic.690421119](https://doi.org/10.1002/aic.690421119).
- [30] Z. Wei, Q. Huang, Edible Pickering emulsions stabilized by ovotransferrin–gum arabic particles. *Food Hydrocolloids*, 89 (2019) 590–601, doi: [10.1016/j.foodhyd.2018.11.037](https://doi.org/10.1016/j.foodhyd.2018.11.037).
- [31] L. Hohl, S. Röhl, D. Stehl, R. von Klitzing, M. Kraume, Influence of nanoparticles and drop size distributions on the rheology of w/o Pickering emulsions. *Chem Ingenieur Technik*, 88 (2016) 1815–1826, doi: [10.1002/cite.201600063](https://doi.org/10.1002/cite.201600063).



- [32] Y. Jia, M. Zheng, Q. Xu, C. Zhong, Rheological behaviors of Pickering emulsions stabilized by TEMPO-oxidized bacterial cellulose. *Carbohydr Polym*, 215 (2019) 263–271, doi: [10.1016/j.carbpol.2019.03.073](https://doi.org/10.1016/j.carbpol.2019.03.073).
- [33] L.G. Torres, R. Iturbe, M.J. Snowden, B.Z. Chowdhry, S.A. Leharne, Preparation of o/w emulsions stabilized by solid particles and their characterization by oscillatory rheology. *Colloids Surfaces A: Physicochem Eng Aspects*, 302 (2007) 439–448, doi: [10.1016/j.colsurfa.2007.03.009](https://doi.org/10.1016/j.colsurfa.2007.03.009).
- [34] C.E.P. Silva, K.C. Tam, J.S. Bernardes, W. Loh, Double stabilization mechanism of O/W Pickering emulsions using cationic nanofibrillated cellulose. *J Colloid Interface Sci*, 574 (2020) 207–216, doi: [10.1016/j.jcis.2020.04.001](https://doi.org/10.1016/j.jcis.2020.04.001).
- [35] L. Kotliarevski, K.A. Mani, R.A. Feldbaum, N. Yaakov, E. Belausov, E. Zelinger, D. Ment, G. Mechrez, Single-conidium encapsulation in oil-in-water Pickering emulsions at high encapsulation yield. *Front Chem*, 9 (2021) 726874, doi: [10.3389/fchem.2021.726874](https://doi.org/10.3389/fchem.2021.726874).
- [36] J.H.J. Thijssen, J. Vermant, Interfacial rheology of model particles at liquid interfaces and its relation to (bicontinuous) Pickering emulsions. *J Phys: Condens Matter*, 30 (2018) 023002, doi: [10.1088/1361-648X/aa9c74](https://doi.org/10.1088/1361-648X/aa9c74).
- [37] S. Reynaert, P. Moldenaers, J. Vermant, Interfacial rheology of stable and weakly aggregated two-dimensional suspensions. *Phys Chem Chem Phys*, 9 (2007) 6463–6475, doi: [10.1039/b710825g](https://doi.org/10.1039/b710825g).
- [38] A. Schröder, J. Sprakel, K. Schroën, J.N. Spaen, C.C. Berton-Carabin, Coalescence stability of Pickering emulsions produced with lipid particles: A microfluidic study. *J Food Eng*, 234 (2018) 63–72, doi: [10.1016/j.jfoodeng.2018.04.007](https://doi.org/10.1016/j.jfoodeng.2018.04.007).
- [39] C. Griffith, H. Daigle, A comparison of the static and dynamic stability of Pickering emulsions. *Colloids Surfaces A: Physicochem Eng Aspects*, 586 (2020) 124256, doi: [10.1016/j.colsurfa.2019.124256](https://doi.org/10.1016/j.colsurfa.2019.124256).
- [40] H. Du Le, S.M. Loveday, H. Singh, A. Sarkar, Pickering emulsions stabilised by hydrophobically modified cellulose nanocrystals: Responsiveness to pH and ionic strength. *Food Hydrocolloids*, 99 (2020) 105344, doi: [10.1016/j.foodhyd.2019.105344](https://doi.org/10.1016/j.foodhyd.2019.105344).
- [41] L.E. Low, S.P. Siva, Y.K. Ho, E.S. Chan, B.T. Tey, Recent advances of characterization techniques for the formation, physical properties and stability of Pickering emulsion. *Adv Colloid Interface Sci*, 277 (2020) 102117, doi: [10.1016/j.cis.2020.102117](https://doi.org/10.1016/j.cis.2020.102117).
- [42] L.E. Low, B.T. Tey, B.H. Ong, E.S. Chan, S.Y. Tang, Palm olein-in-water Pickering emulsion stabilized by Fe<sub>3</sub>O<sub>4</sub>-cellulose nanocrystal nanocomposites and their responses to pH. *Carbohydr Polym*, 155 (2017) 391–399, doi: [10.1016/j.carbpol.2016.08.091](https://doi.org/10.1016/j.carbpol.2016.08.091).
- [43] K. van der Vaart, Y. Rahmani, R. Zargar, Z. Hu, D. Bonn, P. Schall, Rheology of concentrated soft and hard-sphere suspensions. *J Rheol*, 57 (2013) 1195–1209, doi: [10.1122/1.4808054](https://doi.org/10.1122/1.4808054).
- [44] M. McEwan, D. Green, Rheological impacts of particle softness on wetted polymer-grafted silica nanoparticles in polymer melts. *Soft Matter*, 5 (2009) 1705–1716, doi: [10.1039/b816975f](https://doi.org/10.1039/b816975f).
- [45] P. Taylor, Ostwald ripening in emulsions. *Colloids Surfaces A: Physicochem Eng Aspects*, 99 (1995) 175–185, doi: [10.1016/0927-7757\(95\)03161-6](https://doi.org/10.1016/0927-7757(95)03161-6).
- [46] I. Szymańska, A. Żbikowska, K. Marciniak-Łukasiak, Effect of addition of a marine algae (*Chlorella protothecoides*) protein preparation on stability of model emulsion systems. *J Dispersion Sci Technol*, 41 (2020) 699–707. doi: [10.1080/01932691.2019.1611438](https://doi.org/10.1080/01932691.2019.1611438).
- [47] B.A. Khan, Basics of pharmaceutical emulsions: A review. *Afr J Pharm Pharmacol*, 5 (2011) 2715–2725, doi: [10.5897/AJPP11.698](https://doi.org/10.5897/AJPP11.698).

- [48] I.B. Ivanov, K.D. Danov, P.A. Kralchevsky, Flocculation and coalescence of micron-size emulsion droplets. *Colloids Surfaces A: Physicochem Eng Aspects*, 152 (1999) 161–182, doi: [10.1016/S0927-7757\(98\)00620-7](https://doi.org/10.1016/S0927-7757(98)00620-7).
- [49] N.D. Denkov, S. Tcholakova, I.B. Ivanov, B. Campbell, Methods for evaluation of emulsion stability at a single drop level. In Paper included in the Third World Congress on Emulsions, Lyon (2002).
- [50] K. Larson-Smith, A. Jackson, D.C. Pozzo, SANS and SAXS analysis of charged nanoparticle adsorption at oil–water interfaces. *Langmuir*, 28 (2012) 2493–2501, doi: [10.1021/la204513n](https://doi.org/10.1021/la204513n).

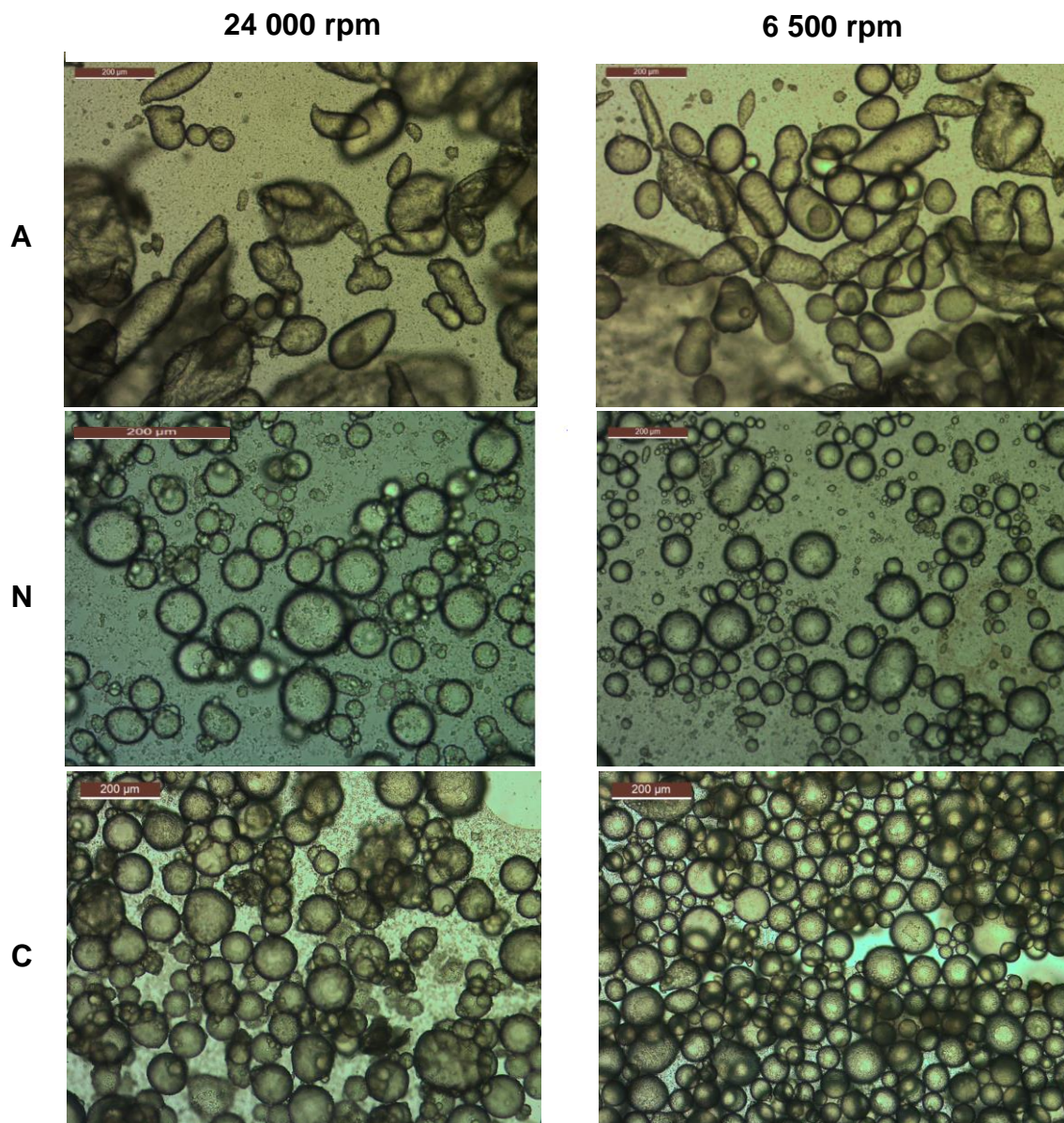
# Supplementary Information

## Rheological properties and stability of Pickering emulsions stabilized with Differently Charged Particles

Mathis Benyaya, Marie-Alexandrine Bolzinger, Yves Chevalier, Claire Bordes

### SI1. Droplets morphology

Optical microscopy pictures revealed the shape of the oil droplets in all the studied emulsions. Oil droplets were nicely spherical for N-, C-, C/N- and A/C(6 500)-emulsions. They were clearly non-spherical for A-emulsions. Intermediate shape with slight asphericity was observed for A/N and A/C(24 000)-emulsions.



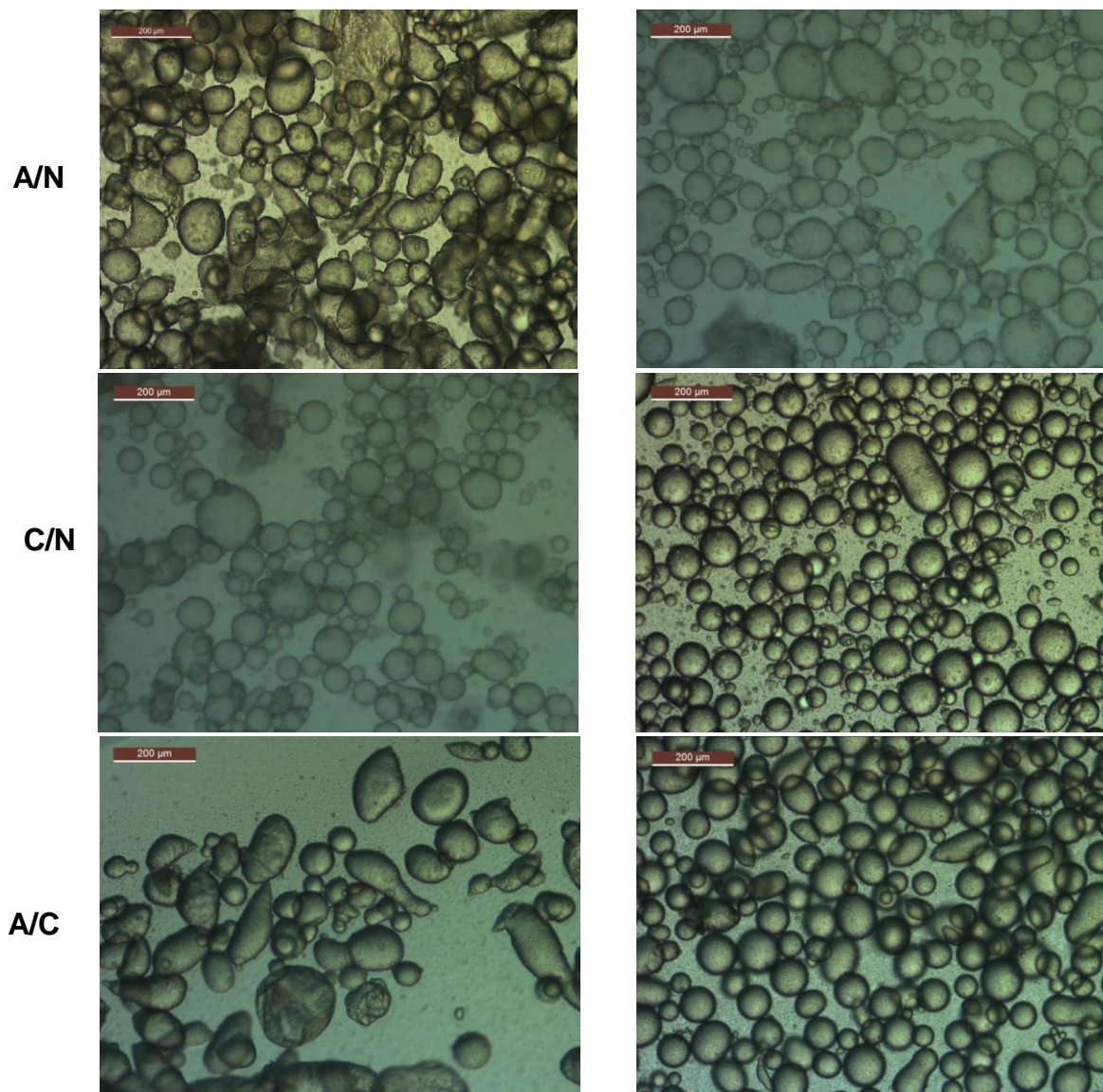


**Figure SII.** Optical microscopy pictures of the emulsions made with 43 mg of particles per  $\text{cm}^3$  of oil. Emulsions prepared at 24 000 rpm are presented in the left column, and the ones prepared at 6 500 rpm in the right column. From top to bottom, A-, N-, C-, A/N-, C/N- and A/C-emulsions. The scale bar is 200  $\mu\text{m}$  in all pictures.

## SI2. Viscosity of the emulsions

Within the studied ranges, the concentration of stabilizing particles and the emulsification process did not influence the rheological behavior. Indeed, no significant difference was found between a same type of emulsion stabilized with different amounts of particles or prepared using different stirring rates.

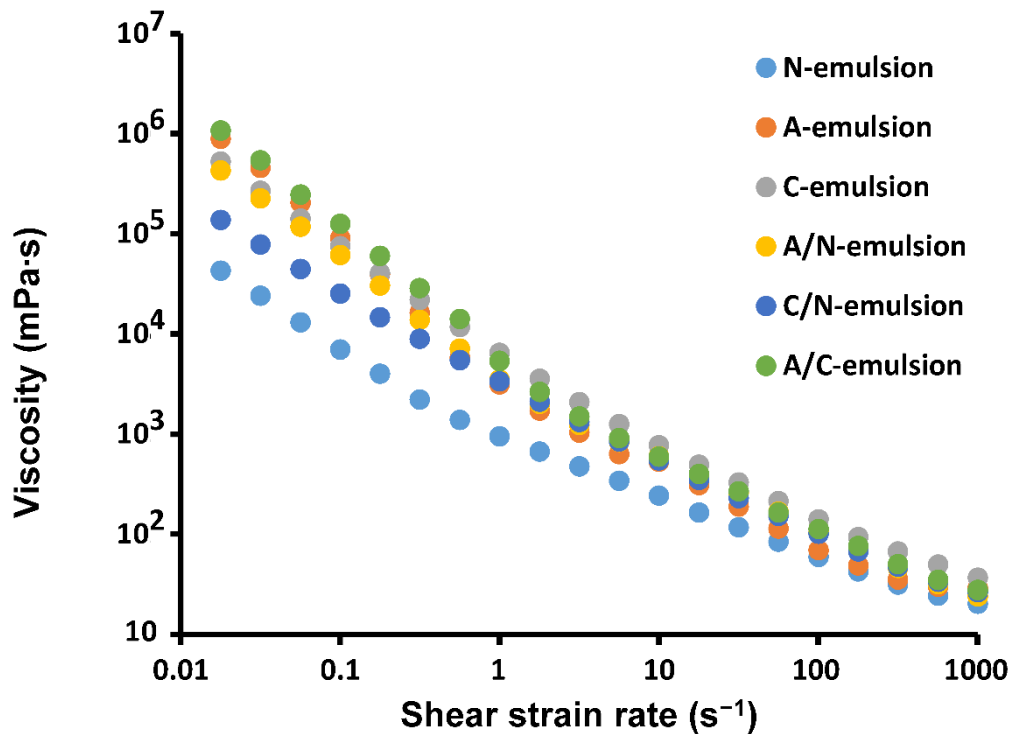


**Figure SI2.** Viscosity of the six types of emulsion. Mean value of measurements for the three particle concentrations and the two stirring rates.

## SI3. Droplets Deformation in a C-emulsion

A sample of emulsion was deposited on a microscope slide and covered with a cover slip. The top slide was then slowly pulled under microscopic observation for making the emulsion flow under shear and the video was recorded. The video file is given as [VideoSI3.mp4](#).